Chemical Engineering Science 269 (2023) 118498

Contents lists available at ScienceDirect

Chemical Engineering Science

journal homepage: www.elsevier.com/locate/ces

Ex-situ biological hydrogen methanation in trickle bed reactors: Integration into biogas production facilities

Donya Kamravamanesh [a,*], Johanna M. Rinta Kanto [a], Harri Ali-Loytty [b], Antti Myllärinen [c], Mikko Saalasti [c], Jukka Rintala [a], Marika Kokko [a]

[a] Faculty of Engineering and Natural Sciences, Materials Science and Environmental Engineering, Tampere University, 33720 Tampere, Finland
[b] Faculty of Engineering and Natural Sciences, Physics, Tampere University, 33720 Tampere, Finland
[c] Doranova Oy, Valkkistentie 2, 37470 Vesilahti, Finland

HIGHLIGHTS

- Digestate and reject water were used as inoculum and trickling liquid in BHM.
- With reject water H_2 loading rate of 10.8 L_{H2} L^{-1}_{Rv} d^{-1} was achieved.
- Relative abundance of *Methanothermobacteriaceae* increased to more than 60%
- Trace element addition is crucial for stable BHM when reject water is used.
- Biodegradation of organic matter in reject water changes the H_2/CO_2 stoichiometry.

GRAPHICAL ABSTRACT

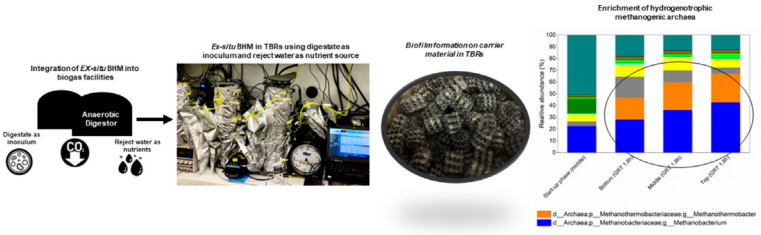

ARTICLE INFO

Article history:
Received 18 November 2022
Received in revised form 11 January 2023
Accepted 16 January 2023
Available online 20 January 2023

Keywords:
Biological hydrogen methanation
Power-to-gas
Digested biowaste reject water
Trickle bed reactor
Hydrogenotrophic methanogens

ABSTRACT

Biological hydrogen methanation (BHM) is a biocatalytic process for biogas upgrading. Integrating *ex-situ* BHM processes into biogas facilities has the advantage of using inoculum, CO_2, and nutrients directly from anaerobic digestion (AD) processes to enhance CH_4 productivity. This study investigated the potential of biowaste digestate as an inoculum and digested biowaste reject water as the trickling liquid and nutrient source in thermophilic trickle bed reactors (TBRs). Use of reject water improved H_2 conversion efficiency to up to 99 %, thus achieving a H_2 loading rate of 10.8 L_{H2} L^{-1}_{Rv} d^{-1} at a gas retention time (GRT) of 1.8 h and CH_4 productivity of 2.6 L L^{-1}_{Rv} d^{-1} implying that reject water contains macronutrients beneficial to enriching hydrogenotrophic methanogens. However, at high H_2 loading rates, a trace element supply was necessary to stabilize process performance. Hydrogenotrophic methanogens *Methanothermobacter* and *Methanobacterium* were selectively enriched, mainly due to the increased H_2 loading rate.

1. Introduction

Power-to-gas technology is a promising platform for converting electricity from renewable energy sources, such as wind and solar, into H_2 via electrolysis (equation 1.1; (Ozturk et al. 2021). Due to the low energy density of H_2, its storage and transportation can be challenging, and conversion to CH_4 is more compatible with the existing gas infrastructure (Thapa et al. 2022). Besides thermo-

* Corresponding author at: Faculty of Engineering and Natural Sciences, Materials Science and Environmental Engineering, Tampere University, P.O. Box 541, FI33101, Finland.
E-mail address: donya.kamravamanesh@tuni.fi (D. Kamravamanesh).

https://doi.org/10.1016/j.ces.2023.118498
0009-2509/

chemical methanation or the Sabatier process, converting H_2 and CO_2 into CH_4 can be done biologically (biomethanation) via biological H_2 methanation BHM; equation 1.2; (Rusmanis et al. 2019). The theoretical stoichiometric ratio of H_2:CO_2 for an optimum biomethanation reaction is 4:1 (Rittmann et al. 2015), though this requires an efficient gas–liquid mass transfer of H_2 to enable H_2/CO_2 availability for microorganisms, and thus a high CH_4 production rate (Rusmanis et al. 2019).

$$2H_2O \rightarrow 2H_2 + O_2$$

$$\Delta G^0 = 285.8 \text{ kJ mol}^{-1} \quad (1.1)$$

$$4H_2 + CO_2 \rightarrow CH_4 + 2H_2O$$

$$\Delta G^0 = -165 \text{ kJ mol}^{-1} \quad (1.2).$$

BHM can be performed in an *ex-situ* process in which a separate reactor is used for the reaction between H_2 and CO_2. Continuous flow *ex-situ* reactor studies have been performed, such as those on trickle bed reactors (TBRs), up-flow reactors (Bassani et al. 2017), continuous stirred tank reactors and bubble column reactors (Kougias et al. 2017), both in laboratories (Porté et al. 2019, Sieborg et al. 2020, Thapa et al. 2022) and in pilot research (Burkhardt et al. 2019, Sieborg et al. 2020). In TBRs, high height-to-diameter ratios allow efficient mass transfer between the three phases present in the reactor, that is, methanogens immobilized on carrier material, gaseous H_2 and CO_2, and nutrients provided via trickling liquid (Sposob et al. 2021). The high surface-to-volume ratio of the carrier material in a TBR enables the cell retention of slow-growing methanogenic archaea in the form of biofilm (Gavala et al. 2021). In BHM reactors, hydrogenotrophic methanogens often prevail (Porté et al. 2019, Dahl Jønson et al. 2020). Competing metabolic routes can coexist, such as homoacetogens that can convert H_2 and CO_2 to acetate, while syntrophic acetate oxidizing bacteria (SAOB) utilize acetate to generate H_2 and CO_2 (Rafrafi et al. 2021). Most studies on *ex-situ* BHM have reported inoculation using pre-enriched microbial communities from laboratory BHM reactors or conditioned cultivation flasks (Luo et al. 2012, Alitalo et al. 2015, Dupnock et al. 2017, Jensen et al. 2019, Maegaard et al. 2019, Porté et al. 2019, Sieborg et al. 2020). Furthermore, in many laboratory studies, researchers have used mineral media as the trickling liquid (Rachbauer et al. 2016, Dupnock et al. 2017, Strübing et al. 2017, Strübing et al. 2018, Burkhardt et al. 2019). In a recent pilot study by Jønson et al. (2022) a mixture of NPK fertilizer and commercial trace element solution were used as trickling liquid and decanted digestate was only utilized as a buffering agent. In *ex-situ* BHM, the H_2 loading rate is an important factor that affects its partial pressure and microbial community composition, as well as CH_4 production rate, reactor size and the application's overall economic feasibility. *Ex-situ* TBRs have also shown high H_2 conversions, up to 99 % (Strübing et al. 2017, Porté et al. 2019, Ashraf et al. 2021). The studied H_2 loading rates were typically in the range of 7.2–11.9 L_{H2} L_{Rv}^{-1} d^{-1} (Porté et al. 2019, Dahl Jønson et al. 2020, Sieborg et al. 2020) but could be as high as 62.1 L_{H2} L_{Rv}^{-1} d^{-1}, as in Strübing et al. (2019), resulting in a CH_4 production rate of 1.7–15.4 L_{CH4} L_{Rv}^{-1} d^{-1}.

One way to render large-scale BHM is to couple it with an existing biogas plant to utilize the CO_2 present in the biogas produced from the anaerobic digestion (AD) of various waste streams, such as sewage sludge or food waste. Besides upgrading CO_2, integration could also enable the use of digestate as an inoculum and reject water as a trickling liquid and nutrient source. The potential of using both digestate and reject water in *ex-situ* BHM has not been widely studied.

Researchers in a few *ex-situ* BHM studies have inoculated both laboratory and pilot TBRs with digestate from a biogas plant (Dahl Jønson et al. 2020), though without major treatment and enrichment steps. One TBR start-up was studied with nutrients and trace elements originating only from inoculum within 50 days (Strübing et al. 2017). While above 90 % CH_4 was obtained on day 7, the addition of sulphide on day 47 was necessary to recover the CH_4 content (from 55 % to 96 %) that had declined since day 25. pH control was also required from day 66 onwards due to decreasing pH value (<6.2) resulting from the increasing H_2 loading rate (Strübing et al. 2017). Another study achieved high CH_4 content (99 %) after 25 days in a BHM, but it was accompanied with a high acetate concentration of 5.8 g L^{-1} during start-up that was linked to the replenishment of the trickling liquid with fresh pasteurized cattle manure (Dahl Jønson et al. 2020). The inoculation of TBRs directly with digestate should be further elucidated to obtain stable long-term BHM, and to find means of controlling acetate production during process start-up.

Digestate or its supernatant (Bassani et al. 2017, Kougias et al. 2017, Porté et al. 2019, Strübing et al. 2019) has been utilized as a trickling liquid to supply macro- and micronutrients in BHM. Many studies extensively pre-treated digestates or cow manure prior to their use as nutrient sources in TBRs. For example, in one study digestate was incubated for more than 3 months to degrade residual organic matter (Porté et al. 2019), while in others, cow manure was pasteurized (Sieborg et al. 2020) and/or followed by various centrifugation and filtration steps (Ashraf et al. 2021). This yielded H_2 loading rates of 7.2–11.9 L_{H2} L_{Rv}^{-1} d^{-1} for CH_4 production rates of 1.7–2.5 L_{CH4} L_{Rv}^{-1} d^{-1} (Porté et al. 2019, Dahl Jønson et al. 2020, Sieborg et al. 2020). Studies on thermophilic BHM using reject water from a biogas plant without pre-treatment are scarce. However, to integrate BHM into biogas plants, reject water without or with minor pre-treatment should be utilized. Thus, more research on understanding the prerequisites of using reject water directly as a trickling liquid in BHM is necessary.

The main aim of this study was to assess whether digestate and reject water from a biogas plant that treats source-separated food waste could be used as a TBR inoculum and trickling liquid, respectively. In addition, the H_2 loading potential of the TBRs was studied in terms of methane production rate via stepwise increase of the H_2 loading rate when using reject water as a trickling liquid. Furthermore, the requirement for additional trace elements at increased H_2 loading rates was assessed, as was the impact of these increased loading rates and reject water on the evolution of microbial community composition in TBRs.

2. Materials and methods

2.1. Inoculum and reject water

The inoculum was digestate from the Stormossen biogas plant (Vaasa, Finland) treating source separated food waste under mesophilic conditions. The reject water obtained from dewatering the digestate was used as the nutrient source and trickling liquid. The digestate and reject water were filtered using a laboratory steel sieving mesh with a 25-μm cut-off to remove larger solid particles, and then passed through cheesecloth to remove smaller particles and precipitates which could block the liquid trickling system. The treated reject water was stored at 4 °C during the experimental period. Prior to usage, the reject water was sparged with nitrogen gas and heated at 55 °C for 30 min to facilitate anaerobic and thermophilic conditions. The characteristics of the digestate and reject water are presented in Table 1. The mineral media used in the Start-up phase was derived from Strübing et al. (2017), with the composition as follows: 7.3 g/L NH_4Cl, 9.0 g/L Na_2CO_3, 0.75 g/L EDTA, 0.3 g/L $MgCl_2{\cdot}6H_2O$, 0.75 g/L $FeCl_2.4H_2O$, 1.5 mg/L

Table 1
The characteristics of inoculum and reject water after sieving and filtration with cheese cloth.

	pH	TS (%)	vS (%)	Ammonium ($g\ L^{-1}$)	VFAs ($g\text{-}COD\ L^{-1}$)	Acetate ($g\text{-}COD\ L^{-1}$)	Soluble COD ($g\ L^{-1}$)	S ($g\ L^{-1}$)	Na ($g\ L^{-1}$)	Mg ($mg\ L^{-1}$)	K ($mg\ L^{-1}$)	Ca ($mg\ L^{-1}$)	Fe ($mg\ L^{-1}$)	P ($mg\ L^{-1}$)	Ni ($mg\ L^{-1}$)	Co ($mg\ L^{-1}$)	Zn ($mg\ L^{-1}$)	Cu ($mg\ L^{-1}$)	Se ($mg\ L^{-1}$)	Mo ($mg\ L^{-1}$)
Digestate	7.7	1.3 ± 0.03	0.8 ± 0	2.4 ± 0.1	2.1 ± 0.0	1.3 ± 0.0	13.2 ± 1	0.2 ± 0.0	1.5 ± 0	60 ± 2	220 ± 1	220 ± 1	7.5 ± 0.1	40 ± 0.2	0.05 ± 0	0.01 ± 0	0.5 ± 0	0	0	0.02 ± 0
Reject water	7.5	1.4 ± 0.01	0.9 ± 0.01	2.3 ± 0.2	1.8 ± 0.0	0.8 ± 0.0	15.3 ± 1	0.16 ± 0.0	1.5 ± 0.2	60 ± 2	218 ± 1	215 ± 1	7.4 ± 0.1	40 ± 0.5	0.05 ± 0	0.01 ± 0	0.5 ± 0	0	0	0.02 ± 0

*Data represents the mean ± standard deviation of three individual measurements.
*Abbreviations: Total Solid (TS), Volatile Solid (VS).
*The digestate and reject water (sieved dewatered digestate) used for this study were not from the same batch performing anaerobic digestion of food waste. Therefore, they showed similar TS/vS content.

$(NH_4)_6Mo_7O_{24}.2H_2O$, 0.1 mg/L $Na_2SeO_3.5H_2O$, 9.0 mg/L $NiCl_2{\cdot}6H_2O$ and 1.5 mg/L $CoCl_2{\cdot}6H_2O$ In addition, K_2HPO_4 and KH_2PO_4 were added to the mineral media as buffering agents for a final concentration of 0.1 M.

2.2. Trickle bed reactor setup

Three parallel polyacrylic TBRs (R1, R2 and *R*3; Fig. 1) with a total volume of 10 L, inner diameter of 0.14 m and height of 0.60 m (H:D ratio of 4.3:1) were operated with the same process parameters. The polypropylene packing rings used as carrier material were Hel-X bio carriers HXF 17KLL (602 $m^2\ m^{-3}$-, Christian Stöhr GmbH, Germany), occupying 8.3 L of trickle bed volume in each reactor. The temperature of the reactors was maintained at 50–55 °C using a circulating hot water jacket heated with a water bath (SUB Aqua 26, Grant, UK). A digital thermometer was installed in the middle of R1 to monitor the temperature.

The TBRs were designed for a counter-current continuous flow of the inlet gas and trickling liquid to elevate mass transfer. The inlet H_2 and CO_2 gas flows (Linde, Finland) were controlled with mass flow controllers (Bronkhorst EL-Flow, YTM, Finland) at a stoichiometric ratio of 4:1 and were moisturized before injection into the reactors. Of note, a small gas leakage mainly of H_2 (ca. 10 % of total inflow gas) was detected in R2 on day 70 due to a small crack, resulting in a slightly lower stoichiometric ratio of H_2:CO_2 inside this reactor compared to the others. The inlet gas diffusion system installed at the bottom of the reactors consisted of four diffusion stones (Humlegardens, Ekolager, Sweden). The gas outlet from the top of the reactors was connected to aluminium gas bags (Supel™ Inert Foil Gas Sampling Bags, Supelco, USA) to collect the outlet gas.

A trickling liquid tank of 2 L was placed in a separate water bath at 55 °C. The liquid was trickled from the top of the reactor at a continuous optimized flow rate of 75 mL min^{-1} using a circular distributor shower with 10 ports, each port having a diameter of 2 mm. To evenly distribute the trickling liquid in the reactors, two sizes of glass beads (10 and 20 mm in diameter) occupied 3 cm on top of the carrier material. A pH probe (Orbisint CPS11D, Endress + Hauser, Germany) was installed in the liquid circulation line of all reactors to continuously recording pH values using an eight-channel transmitter (Liquiline CM448, Endress + Hauser, Germany).

2.3. Process set-up

All three reactors were operated for 192 days (Table 2). The study was divided into three phases: Start-up (0–108 days), Adaptation (108–131 days) and Experimental (132–192 days). For the Start-up phase, mineral media was used as the trickling liquid (total volume of 2 L) and amended with the inoculum at 80:20 (V/V) % ratio corresponding to 0.16 % volatile solid.

During the Adaptation phase, the mineral media used as the trickling liquid and amended with inoculum was replaced with reject water in two steps by replacing 1 L of the trickling liquid tank content with reject water on days 108 and 122. On day 132, the Experimental phase started. At this time, the H_2 loading rate was increased and the addition of trace elements was studied between days 149 and 157. Five different H_2 loading rates were studied, with the rate changed once steady state conditions were obtained (i.e. when CH_4 production rate (r_{CH4}) changed to < ± 0.1 L d^{-1} for at least 5 days in a row in each individual reactor).

To ensure buffering capacity, the prevention of nutrient limitations and identical starting points before increasing each H_2 loading rate, 1 L of the trickling liquid tank content was replaced with fresh reject water on days 143, 164, 173 and 185. The impact of the various trace elements on methane content and production

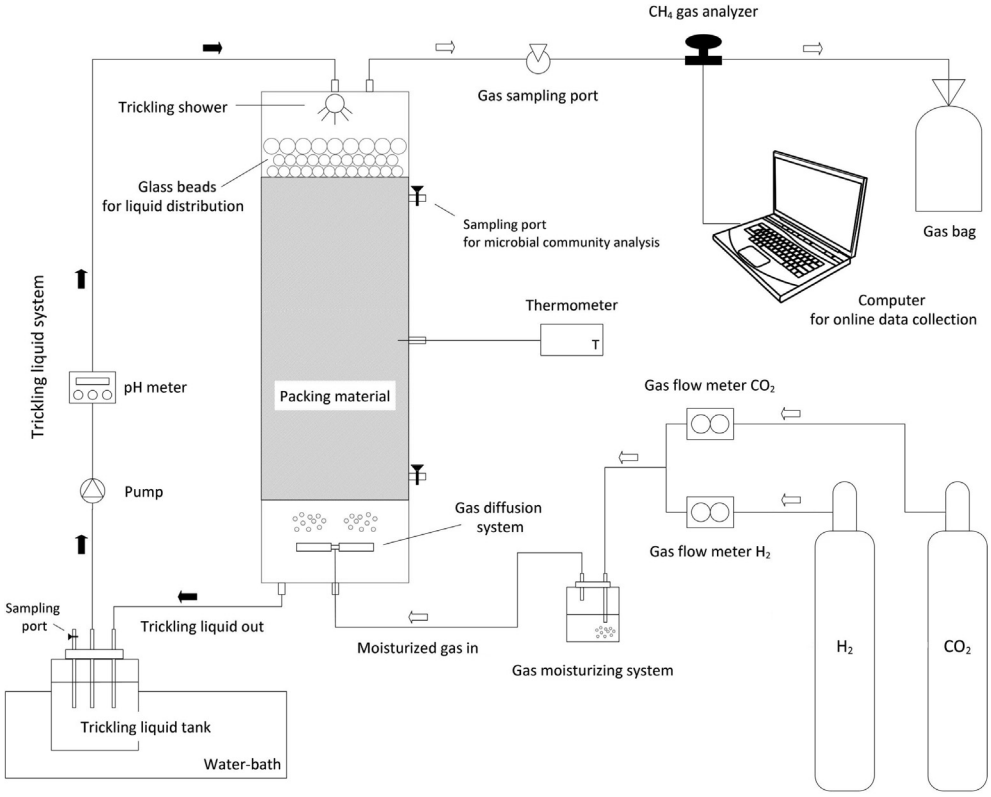

Fig. 1. A schematic representation of the thermophilic TBRs set-up for BHM.

Table 2
The H_2 and CO_2 flow rates, gas retention times (GRTs) and time periods of the three distinct process phases.

Process phase	H_2 flowrate ($L\ L_{Rv}^{-1}\ d^{-1}$)	CO_2 flowrate ($L\ L_{Rv}^{-1}\ d^{-1}$)	GRT (h)	Run time (days)
Start-up phase	1.5	0.37	12.8	0–108
Adaptation phase	1.5	0.37	12.8	108–132
Experimental phase	2.6	0.65	7.4	132–146
	4.1	1.03	4.7	146–170
	6.0	1.5	3.2	170–178
	8.2	2.05	2.3	178–188
	10.8	2.7	1.8	188–192

rate was studied accordingly. On day 149, a trace element solution derived from Strübing et al. (2017) was also used in the symineral media for reactor start-up, with a final concentration of 5 mg/L $ZnSO_4{\cdot}7H_2O$, 5 mg/L $MnCl_2{\cdot}4H_2O$, 4 mg/L $CuCl_2{\cdot}5H_2O$ and 0.4 mg/L $Na_2WO_4{\cdot}2H_2O$ On day 151, trace elements $FeCl_2{\cdot}4H_2O$ (50 mg/L), $NiCl_2{\cdot}6H_2O$ (1.5 mg/L) and $CoCl_2{\cdot}6H_2O$ were added, and on day 157 $(NH_4)_6Mo_7O_{24}.2H_2O$ (0.5 mg/L) and $Na_2SeO_3{\cdot}5H_2O$ (100 μg L^{-1}) were added to the trickling liquid tank. Based on the obtained results, on process days 164, 173 and 185 a mixture of trace element solutions containing Fe, Mo, Se, Ni and Co (in the above-mentioned concentrations) was added to the reject water.

2.4. Analytical methods and calculations

Total solids, volatile solids and soluble chemical oxygen demand (COD) were measured following the standard method (APHA, 2018a) and dichromate method (APHA, 2018b). The liquid samples for the analysis were collected from trickling liquid tank and the analysis was done after centrifugation (4500 rpm, 15 min: Rotina 420) and filtration (pore size 0.45 μm, Chromafil, Macherey-Nagel, Germany). All analyses were performed for at least duplicate samples. VFA concentration was measured with a gas chromatograph (Shimadzu Ordior GC-2010 plus) with a ZB-WAX Plus column (Phenomenex, USA) using a flame ionization detector, as described by Kokko et al. (2018). VFA concentrations were converted to COD values to present individual VFAs and calculate total VFA. Cations were determined using ion chromatography with Dionex DX-120 (ThermoFisher Scientific, USA) and a Dionex Ionpac™ CS12A column guarded with an Ionpac™ CG12A pre-column (ThermoFisher Scientific, USA) and further equipped with an AS40 autosampler. The methane concentration in the outlet gas was monitored using online BCP-CH_4 sensors (BlueSens, Germany). The outlet gas composition was analysed off-line using a GC-2014 (Shimadzu, USA) fitted with a 6Ft 1/8 2 mm (Porapak N 80/100 Ni, Agilent Technologies, CA, USA) equipped with a thermal conductivity detector. Nitrogen acted as the carrier gas at a flow rate of 20 mL min^{-1}, column oven temperature of 80 °C and detector temperature of 110 °C. The volume of gas col-

lected in the gas bags was determined using the water-displacement method according to Owen et al. (1979), at standard temperature and pressure.

Elemental concentrations were measured via inductively coupled plasma mass spectrometry (ICP-MS) using Thermo Scientific iCAP™ RQ equipment. All measurements were performed in kinetic energy discrimination (KED) mode using He as the collision gas in the collision/reaction cell and Ar as the carrier gas.

Gas retention time (GRT) was calculated based on the total inlet gas flow rate ($F_{H2+CO2,in}$-; L $L_{Rv}^{-1}h^{-1}$), following equation (2.1) (Sieborg et al. 2020):

$$GRT = \frac{24}{F_{H2+CO2}^{in}} \quad (2.1)$$

The CH_4 yield percentage against the inlet gas components H_2 and CO_2 was calculated according to equations (2.2) and (2.3):

$$Y_{CH4/CO2} = \frac{C_{CH4,out}}{C_{CO2,in}} * 100 \quad (2.2)$$

$$Y_{CH4/H2} = \frac{C_{CH4,in}}{C_{H2,in}} * 0.25 * 100 \quad (2.3)$$

where $C_{CH4,out}$ is the flow rate of CH_4 in the outlet gas (L/d), and $C_{H2,in}$ and $C_{CO2,in}$ are the inlet gas flow rates of H_2 and CO_2, respectively (L d^{-1}).

The conversion efficiency (CE) of the inlet gases (H_2 or CO_2) was calculated based on equation (2.4):

$$CE = \frac{F_{in}C_{in} - F_{out}C_{out}}{F_{in}C_{in}} * 100 \quad (2.4)$$

where F_{in} and F_{out} are the gas inlet and outlet flow rates, respectively, while C_{in} and C_{out} are the H_2 or CO_2 percentages in the inlet or outlet gases, respectively. Data were reported at standard temperature and pressure.

2.5. Microbial community analysis

The enrichment of the microbial populations in the TBRs were monitored through planktonic and biofilm samples, with the inoculum sampled after digestate filtration. For the planktonic samples, at the end of the Start-up and Adaptation phases, and at the end of each H_2 loading rate before the addition of fresh reject water, a 50-mL sample was collected from the trickling liquid tank. The samples were centrifuged (4500 rpm, 15 min: Rotina 420) and the resulting pellets stored at −80 °C until further analysis. The biofilm samples were collected at the end of the Start-up phase from the middle of the reactor through a side port using a plastic spatula, and stored at −80 °C. In addition, at the end of the whole process (day 192), the reactors were opened, and carrier materials were collected from their different depths (top, middle and bottom). To remove the biofilm, the carrier materials were washed and sonicated (sonication bath SUB Aqua 2, Grant, UK) with 100 mM of a phosphate buffer (pH 7.4) at room temperature for 5 min, then centrifuged. The pellet was directly used for genomic DNA extraction with the Powersoil® DNA isolation kit (MO BIO Laboratories Inc., CA, USA) according to the manufacturer's recommendations. The purified DNA pellet was re-suspended in DNase-free MQ water and quantified using a Nanodrop 1000 (ThermoFisher Scientific, USA). Microbial community composition was characterized using the V4 region of the 16S rRNA gene. The amplicon libraries were prepared using universal primers 515F/806R with a 5′-3′ sequence of (GTGCCAGCMGCCGCGGTAA/ GGACTACHVGGGTWTCTAAT) and sequenced at a depth of 100 K using Illumina Novaseq, PE250 at Novogene, UK.

Microbiome bioinformatics were carried out using Qiime 2 version 2021.4 (Bolyen et al. 2019) and the details for the data analysis is given in material and methods in the supplementary file.

The amplicon sequences obtained during this study were deposited at the European Nucleotide Archive under project accession number PRJEB53513. After quality filtering, the amplicon data consisted of 5,399,197 sequences and 3136 features (ASVs) from 37 samples.

3. Results

3.1. Process performance in trickle bed reactors

3.1.1. TBR start-up with digestate as inoculum

TBRs were started with digestate from the biogas plant as inoculum (after simple sieving and cloth filtration) and mineral media as trickling liquid. The H_2 and CO_2 loading rates were maintained at 1.5 and 0.37 L L_{Rv}^{-1} d^{-1}, respectively, corresponding to a GRT of 12.8 h. In the beginning of the runs, the reactor temperature fluctuated between room temperature and 55 °C, resulting in decreases in CH_4 content (data not shown here). Thus, the data for the first 30 days of the process was excluded. To provide nutrients for the microbes, accelerate the biofilm formation of the favourable microbial communities and dilute the VFA concentration, 1 L of the trickling liquid tank content was replaced with a mixture of inoculum and mineral media (at a 20:80 (V/V) % ratio) on process days 39, 66, 76, 87 and 95. After day 70, the CH_4 content in the outlet gas reached at least 50 % in all three reactors and increased to approximately 80 % near day 100. During the last 13 days of the Start-up phase, the average CH_4 content in the reactors' outlet gas was 76.4 ± 5 %, with an average CH_4 production rate of 0.39 ± 0.01 L L_{Rv}^{-1} d^{-1} (Fig. 2**a**). In all reactors, pH rose from 7.5 ± 0.1 in the beginning of the run to 8.6 ± 0.2 in R1 and *R*3 once a steady state was reached (Fig. 2**b**). The pH in R2 stabilized at a lower level (8.4 ± 0.1), likely due to higher dissolved CO_2 in the system given the minor H_2 leak in this reactor (Fig. 2**b**). This was also visible in R2′s CO_2 conversion efficiency (Fig. S1**a**).

The average H_2 and CO_2 conversion efficiencies in all three reactors while in a steady state were 95.8 ± 4 % and 89 ± 1.5 %, respectively, while the CH_4 yield (calculated against fed H_2) was higher, approximately 99 % (Fig. 2**c and S1**). During the Start-up phase an increase in total VFA concentrations was detected in all reactors, up to 4.4 g-COD L^{-1} in R1, 3.4 g-COD L^{-1} in R2 and 2.8 g-COD L^{-1} in *R*3 by day 57 (Fig. 3**a**). Acetate was the main VFA, and in R2 and *R*3 it reduced by the end of the Start-up phase from a maximum of 2.4 g-COD L^{-1} to 0.2 and 1.5 g L^{-1}, respectively; the value remained higher in R1 at 3.4 g-COD L^{-1}. In addition, butyrate (0–760 mg-COD L^{-1}), isobutyrate (0–410 mg-COD L^{-1}) and propionate (60–750 mg-COD L^{-1}) were observed in all reactors, with increasing concentrations towards the end of the process start-up. VFA accumulation, particularly acetate, of up to 3.6 g-COD L^{-1} (day 63 in R1) was also revealed by the microbial community characterization, indicating an increase in relative abundance of hydrolytic and acidogenic bacteria (see section 3.2).

3.1.2. Fast adaptation to reject water

The Adaptation phase allowed the study of the reject water's effects on process performance after it partially replaced the mineral media on days 108 and 122, with the H_2 loading rate remained at 1.5 L L_{Rv}^{-1} d^{-1}. After both replacements, the average CH_4 content obtained in R1 and *R*3 (days 108–122) increased to 87 ± 2 % (Fig. 2**a**), with a CH_4 production rate of 0.42 ± 0.02 L L_{Rv}^{-1} d^{-1} The average CH_4 content in R2 remained fairly stable at 73 ± 2 %, with a CH_4 production rate of 0.34 ± 0.02 L L_{Rv}^{-1} d^{-1}. The H_2 and CO_2 conversions in all reactors were 98 ± 2 % and 88.5 ± 1 %, respectively,

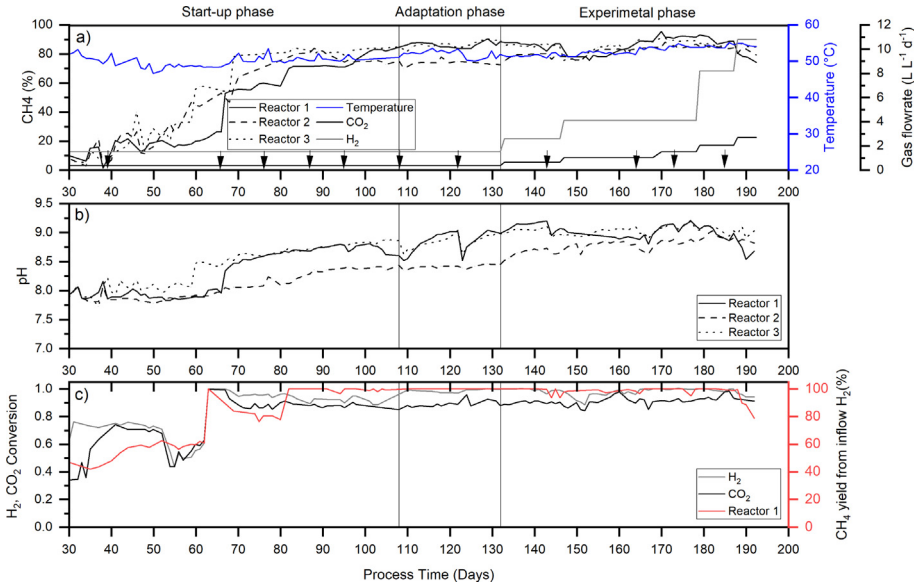

Fig. 2. (a) the methane content, reactor temperature and gas flow rate of H_2 and CO_2; arrows indicate changes made to the trickling liquid. b) pH values of the three TBRs performing BHM. c) The H_2 and CO_2 conversion efficienciesand methane yield of the H_2 inflow in R1.

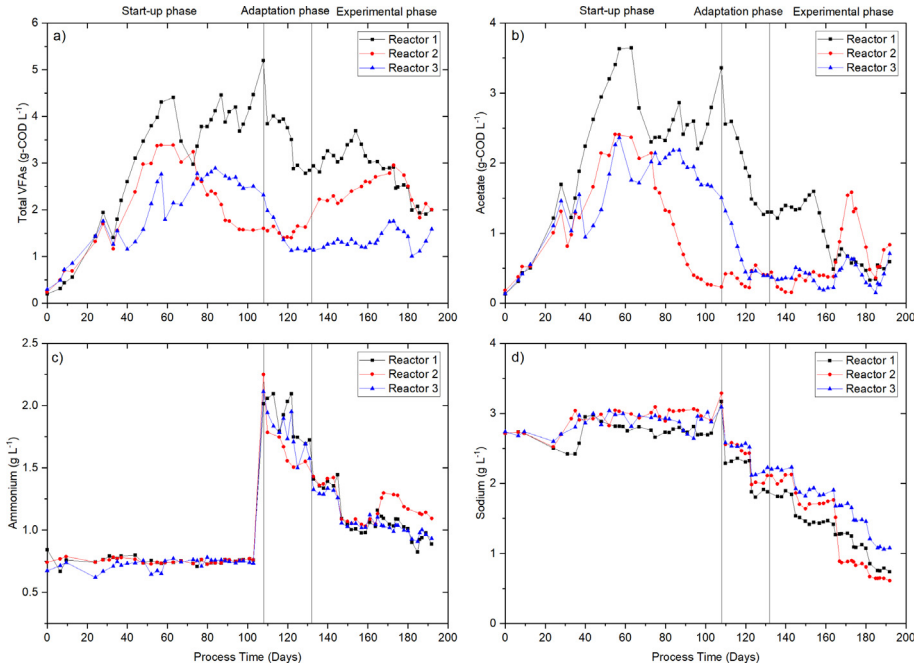

Fig. 3. Concentrations of a) total volatile fatty acids (total VFAs), b) acetate, c) ammonium and d) sodium in the reject water used as a trickling liquid in the TBRs for BHM over process time.

and the average CH_4 yield was 98.2 %. Switching to reject water in this study led to constant pH increments in all reactors: In R1 and *R*3, pH increased from 8.6 ± 0.2 to 8.9 ± 0.05, while that in R2 remained slightly lower (8.4 ± 0.03; Fig. 2**b**). However, no negative effects on methanogens were detected even at pH values of greater than 9.0, which were reached on day 129 in R1 and on day 122 in *R*3.

The acetate concentration reduced significantly in R1 and *R*3 from 3.4 and 1.5 g-COD L^{-1} to 1.3 and 0.4 g-COD L^{-1}, respectively, while in R2 it remained between 0.2 and 0.5 g-COD L^{-1} (Fig. 3**a and b**). Increased concentrations of NH_4-N and Na in the trickling liquid from 0.8 and 2.7 g L^{-1} to 2.1 ± 0.1 and 3.2 ± 0.2 g L^{-1}, respectively on day 108 were due to the mineral media's replacement (1 L) with reject water. After day 108, however, a decrease in both NH_4-N and Na in the trickling liquid to 1 ± 0.1 and 0.8 ± 0.2 g L^{-1}, respectively occurred (Fig. 3**c and d**). Decreased NH_4-N might thus be associated with ammonia stripping in TBRs.

3.1.3. *Effect of H_2 loading rate and impact of trace element addition*

During the Experimental phase, the effect of the H_2 loading rate on the BHM process was studied via stepwise reduction of the GRT from 7.4 to 1.8 h, resulting in the H_2 loading rate increasing from 2.6 to 10.8 L_{H2} L_{Rv}^{-1} d^{-1}. Each experimental stage lasted 8–14 days, except for the GRT of 4.7 h, which lasted for 24 days to study the effects of trace element additions. With the increased H_2 loading

Table 3
Individual TBR performance during Experimental phase.

	Experimental Phase (Days 132–192)												
	GRT 7.4 h (Days 132–146)			GRT 4.7 h (Days 146–170)			GRT 3.2 h (Days 170–178)			GRT 2.3 h (Days 178–188)			GRT 1.8 h (Days 188–192)		
H_2 loading rate (L_{H2} L_{Rv}^{-1} d^{-1})	2.6			4.1			6.0			8.2			10.8		
CO_2 loading rate (L_{CO2} L_{Rv}^{-1} d^{-1})	0.65			1.03			1.5			2.05			2.7		
	R1	R2	*R3*	R1	R2	*R3*	R1	R2	*R3*	R1	R2	*R3*	R1	R2	*R3*
CH_4 content (%)	87 ± 0.92	80 ± 1.5	86 ± 1.3	82 ± 2.2	83 ± 1	87 ± 2	91 ± 0.6	86 ± 1.4	89 ± 1.5	89 ± 2.3	84 ± 2	87 ± 0.8	75 ± 3.8	82 ± 2.4	86 ± 1.1
pH	9.1 ± 0.1	8.6 ± 0.1	9.02 ± 0.1	8.9 ± 0.1	8.8 ± 0.1	9.0 ± 0.2	9.1 ± 0.1	8.8 ± 0.0	9.1 ± 0.1	8.9 ± 0.2	8.9 ± 0.1	9.0 ± 0.1	8.7 ± 0.1	8.9 ± 0.0	9 ± 0.1
CH_4 production rate (L_{CH4} L_{Rv}^{-1} d^{-1})	0.75 ± 0.0	0.52 ± 0.0	0.7 ± 0.1	1.1 ± 0.1	0.9 ± 0.1	1.0 ± 0.0	1.7 ± 0.1	1.5 ± 0.1	1.5 ± 0.1	2.3 ± 0.0	2 ± 0.1	2.1 ± 0.1	2.6 ± 0.2	2.7 ± 0.1	2.6 ± 0.3
H_2 conversion efficiency (%)	99 ± 1.3	100 ± 0.3	99 ± 1	97 ± 3	100 ± 1	98 ± 2	100 ± 0.4	100 ± 0.3	100 ± 0	98 ± 1.0	100 ± 0	99 ± 0.8	95 ± 1	99 ± 0.3	99 ± 0.3
CO_2 conversion efficiency (%)	90 ± 1	90 ± 2	91 ± 1	91 ± 3	92 ± 2	91 ± 1.8	92 ± 1	92 ± 1	93 ± 1	94 ± 2	93 ± 1	92 ± 1	92 ± 1	92 ± 0	91 ± 1

*The values provided for the individual reactors are represented as the average steady state values ± standard deviation for each GRT.

rate, the CH_4 production rate in R2 improved, though that in all three reactors was comparable (Table 3). The average CH_4 production rate increased from 0.65 ± 0.1 to 2.6 ± 0.1 L_{CH4} L_{Rv}^{-1} d^{-1} upon the increase of the H_2 loading rate from 2.6 to 10.8 L_{H2} L_{Rv}^{-1} d^{-1}. A H_2 conversion efficiency of 98–100 % and CH_4 yield close to 100 % were obtained up to a H_2 loading rate of 8.2 L_{H2} L_{Rv}^{-1} d^{-1}, while the conversion efficiency for CO_2 was between 90 % and 93 %. Reduced H_2 and CO_2 conversion efficiencies were observed at a H_2 loading rate of 10.8 L_{H2} L_{Rv}^{-1} d^{-1} in all reactors. H_2 conversion efficiency in particular reduced from 99 % to 97 %, with a simultaneous decrease in pH from 9 ± 0.1 to 8.8 ± 0.2. pH otherwise remained in the range of 8.6 to 9.1 for the entire experimental phase.

On day 146, when the GRT was decreased from 7.4 h to 4.7 h, the methane content showed an unexpected decline (Fig. 2**a**). To check trace element deprivation, various combinations of trace elements were added to the trickling liquid tank of all reactors. The addition of trace elements (Zn, Cu, W and Mn) on day 149 showed no instant increase in CH_4 content, but after the addition of the trace elements Fe, Ni and Co on day 151 and Mo and Se on day 157, the CH_4 content in all reactors increased stepwise from 76 to 78 % to 84–90 % by day 160. Thus, the combination of trace elements Fe, Ni, Co, Mo and Se was added to the trickling liquid to keep their concentrations stable (Fig. 4) for the rest of the study.

3.2. Evolution of microbial communities

The changes in each reactor's planktonic microbial community compositions were studied via sampling during the Start-up, Adaptation and/or Experimental phases to determine the average relative abundance of their phyla (Figs. 5 **and** S5). The microbial community composition of the inoculum included 25 % archaea, 28 % bacteria and 47 % others, including all taxa with a relative abundance of < 1 %. During the Start-up and Adaptation phases, the microbial community composition in the planktonic samples included on average 27 % and 31 % archaea and 51 % and 49 % bacteria, respectively (Fig. 5**a**), while during the Experimental phase the archaea increased from 31 % to 60 % and bacteria decreased from 49 to 27 %. Simultaneously, the H_2 loading rate increased from 2.6 to 10.8 L_{H2} L_{Rv}^{-1} d^{-1} (reduced GRT from 7.4 h to 1.8 h; Fig. 5**a**). Thus, a stepwise increase in H_2 loading rate appears to be an efficient method for selectively enriching methanogenic archaea.

The PCoA based on Bray-Curtis dissimilarity showed clear differences in the composition of the planktonic and biofilm microbial communities during the use of mineral media (Start-up phase) and reject water (Adaptation and Experimental phases; Fig. S2**a**). In the planktonic samples, Pielou's evenness was significantly higher with mineral media than with reject water (**Fig. S3**). Higher evenness for mineral media indicates a similar abundance of the observed communities, and a shift to lower evenness during reject water usage reflects the selection of fewer organisms (Fig. 5). In the biofilm samples, Pielou's evenness and richness (as indicated by the observed ASVs) were significantly higher after the Experimental phase than after the Start-up phase ($p < 0.05$; **Fig. S4**). With respect to beta diversity, in both the biofilm and planktonic samples a change in trickling liquid from mineral media to reject water was associated with significant differences in microbial community composition (PERMANOVA $p < 0.01$; **Fig. S2**).

Both the planktonic and biofilm archaeal community compositions changed in all reactors (Fig. 5**a and 5b**) over the process. *Methanothermobacter* was the dominant archaeal species in the inoculum, with 22 % relative abundance compared to 2.6 % for *Methanobacterium*. During the Start-up phase, *Methanobacterium* became the dominant archaeal phyla in both the planktonic and biofilm samples, with an average relative abundance of 25 ± 13 % and 21 ± 14 %, respectively in all reactors. In contrast, the average relative abundance of *Methanothermobacter* was below 7 %. During

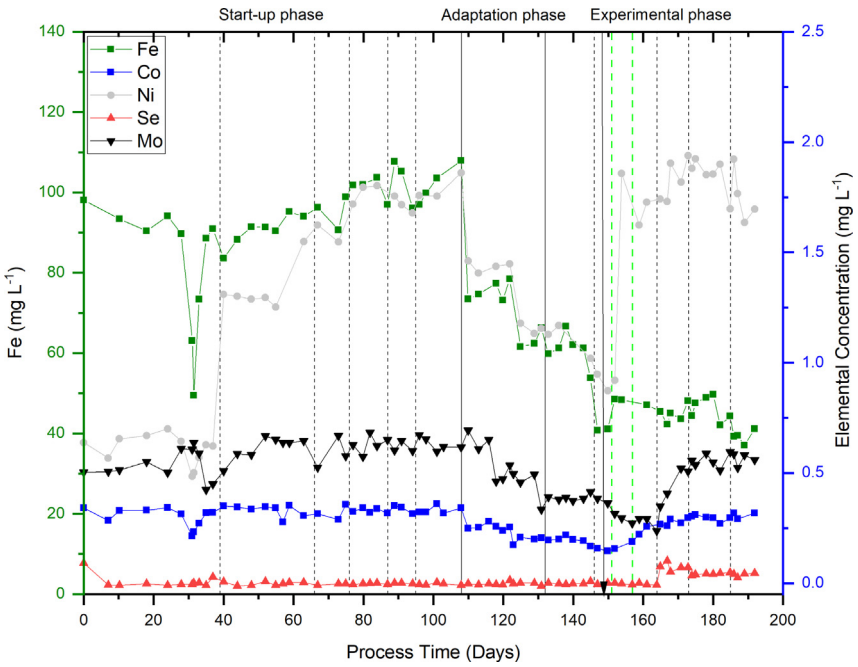

Fig. 4. The concentration of trace elements in the reject water used as a trickling liquid in R1 over process time. The dotted lines represent each refreshment of trickling liquid with mineral media (before day 108) or reject water (after day 108). The arrow represents the addition of Zn, Cu, W and Mn on day 149. The green dotted lines represent the trace elements' addition to the trickling liquid. Fe, Ni and Co were added on day 151 and Mo and Se on day 157. (For interpretation of the references to colour in this figure legend, the reader is referred to the web version of this article.)

the Adaptation phase the microbial community was still evolving and the relative abundance of hydrogenotrophic methanogens (*Methanothermobacter* and *Methanobacterium*), mainly *Methanobacterium*, in the planktonic samples increased slightly, reaching an average value of 31 ± 12 %. During the Experimental phase, with an increase in H_2 loading rate came a significant rise in the relative abundance of hydrogenotrophic methanogens by up to 60 ± 5 % in the planktonic samples (Fig. 5**a**)**.** At the end of the runs, the average total relative abundance of hydrogenotrophic archaea in the biofilm samples at the top of the reactor was 67 ± 6 %, followed by the middle at 58 ± 12 % and the bottom at 47 ± 3 % (Fig. 5**b**).

The bacterial community composition changed in both the planktonic and biofilm samples over the BHM process (Fig. 5). The bacterial community in the inoculum at the genus level mainly consisted of *Defluviitoga*, MBA03 and *Acetomicrobium*, with a total relative abundance of 28 % (Fig. 5**a**). During the Experimental phase, *Defluviitoga* was one of the main genera in the planktonic samples, the relative abundance of which was on average between 11 % and 19 %, except at H_2 loading rates of 4.1 and 8.2 L_{H2} L_{Rv}^{-1} d^{-1}, when its relative abundance increased to 27 ± 10 % and 25 ± 7 %, respectively (Fig. 5**a**). At the end of the run, the average relative abundance of *Defluviitoga* species in the biofilm was 18 ± 7 % at the bottom of the reactors, 10 ± 15 % in the middle and 5 ± 2 % at the top (Fig. 5**b**). The relative abundance of genus *Acetomicrobium* in planktonic cells remained on average between 4 % and 9 %, except at the H_2 loading rate 2.6 L_{H2} L_{Rv}^{-1} d^{-1}, when it increased to 24 %. In the biofilm samples, the relative abundance of *Acetomicrobium* was 0.4–3 %. The relative abundance of genus MBA03 in the planktonic samples varied only slightly between 13 ± 3 % and 16 ± 6 % (Fig. 5**a**).

4. Discussion

4.1. Reactor start-up and adaptation to reject water

An average CH_4 content of 76.4 ± 5 % and a CH_4 production rate of 0.39 ± 0.01 L L_{Rv}^{-1} d^{-1} were obtained in 108 days with a H_2 loading rate of 1.5 L L_{Rv}^{-1} d^{-1} when digestate was used as inoculum. In the present study, the temperature fluctuated during the first 40 days of the Start-up phase, which explained the low H_2/CO_2 conversion efficiencies by day 40. Furthermore, the VFA concentration increased, for instance, acetate by up to 3.6 g-COD L^{-1} near day 60, which could be due to the temperature fluctuations or the conversion of residual organic matter in the digestate to VFAs. During the Start-up phase, hydrolytic bacteria, such as *Clostridia*, were present that could be responsible for VFAs forming from the organic matter in the digestate used as inoculum as well as for chain elongation with H_2 as electron donor (Baleeiro et al. 2021). The results indicate that acetate was not reduced via methanogenesis but oxidized to H_2/CO_2 via syntrophic acetate oxidation (Fig. 3**b and 5**). Thus, the temperature fluctuations and VFA accumulation could have resulted in enriched unfavourable microbial communities. Therefore, five reinoculations were done to increase the chance of enriching the hydrogenotrophic methanogenic archaea and diluting the VFA producing communities in the trickling liquid.

Even though there is no standard definition for TBR start-up, including the target parameters and process performance, some comparison can be made after this phase. In thermophilic TBRs inoculated directly with sieved digestate, shorter start-up times of 50 days have been reported after the addition of sulphide as a sulphur source with a CH_4 content of 99.1 ± 1.3 % and CH_4 production rate of ca. 1.7 ± 0.0 L L_{Rv}^{-1} d^{-1} under a H_2 loading rate of 6.6 L L_{Rv}^{-1} d^{-1} (Strübing et al. 2017). Additional studies have also described a start-up time of 25 days with a 9.9 L L_{Rv}^{-1} d^{-1} H_2 loading rate and an approximately 1.0 L L_{Rv}^{-1} d^{-1} CH_4 production rate when utilizing digestate as inoculum (Dahl Jønson et al. 2020, Ashraf et al. 2021). In the present study, the start-up was prolonged, likely due to the temperature fluctuations and VFA accumulation, indicating that the start-up process can be further improved.

The shift to reject water was straightforward, despite high content of VFAs (1.8 g-COD L^{-1}), soluble CODs (15.3 ± 1 g-COD L^{-1}) and ammonium (2.5 ± 0.15 g L^{-1}). The reject water exhibited no inhibitory effects on process performance in terms of H_2 conversion to CH_4. Furthermore, the increased H_2 conversion efficiencies and

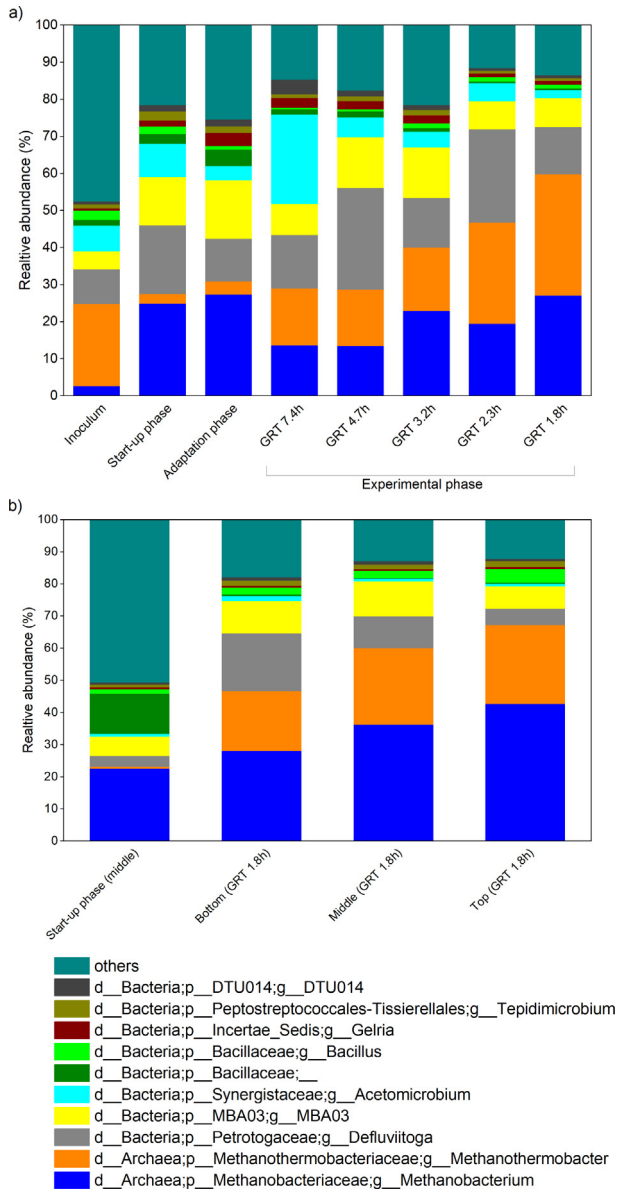

Fig. 5. The average relative abundance of the three individual TBRs performing BHM a) for a microbial community of planktonic samples at the end of the Start-up, Adaptation and Experimental phases with various H_2 loading rates, and b) for biofilm samples collected at the end of the Start-up phase (day 108) from carrier material located at the middle of the reactors and at the end of the process (day 192) from carrier material located at different reactor depths.

CH_4 yields from H_2 indicated that the reject water may supply crucial macronutrients required for the growth of methanogenic archaea. One study has told that sulphide and ammonium (Ashraf et al. 2021) are crucial for *ex-situ* BHM. Ammonium was present in the mineral media used in this study, but sulphide was not added. Based on the current observations, TBR start-up could likely be done with reject water instead of mineral media. However, the need for trace elements, as discussed in **4.2**, should be considered. Additionally, ammonium concentrations of 2.4–4 g L^{-1} have been reported for digestates originating from laboratory-scale biogas reactors that treat food waste (Tampio et al. 2014). Therefore, the feasibility of other digestates and reject water in BHM processes must be investigated. Some inoculum and reject water pre-processing was also considered necessary to prevent technical challenges in a laboratory-scale TBR set-up, though it is possible that industrial-scale cultivation requires little to no processing.

4.2. Increased CH_4 production rate with enhanced H_2 loading rate

In this study, the maximum CH_4 production rate of 2.6 L L_{Rv}^{-1} d^{-1} for *ex-situ* thermophilic BHM in TBRs was obtained with the highest H_2 loading rate of 10.8 L_{H2} L_{Rv}^{-1} d^{-1} (GRT of 1.8 h) when using reject water from digested food waste as a trickling liquid. This CH_4 production rate is higher than in studies where thermophilic BHM was done using digestate as a nutrient source (i.e. a trickling liquid; Table 4). The results obtained in this study are only compared with similar studies performing BHM at thermophilic conditions using digestate as inoculum and/or digestate reject water or another waste stream as nutrient source (Table 4). Still, some studies have reported higher methane production rates at higher H_2 loading rates than in this one. For example, Strübing et al. (2017) described a CH_4 production rate of 15.4 L_{CH4} L_{Rv}^{-1} d^{-1} with a H_2 loading rate of 62.1 L_{H2} L_{Rv}^{-1} d^{-1} using mineral media as a nutrient source. In turn, with a H_2 loading rate of 9.9 L L_{Rv}^{-1} d^{-1}, like in this study, their study's CH_4 production rate was approximately 2.5 L_{CH4} L_{Rv}^{-1} d^{-1}. High H_2 loading rates – up to 62.1 L_{H2} L_{Rv}^{-1} d^{-1} – accompanied with a high volumetric methane production rate were enabled after adapting the buffer, nutrient and trace element supplies to higher H_2 loading rates, taking into account the dilution caused by the water production (Strübing et al. 2017). The maximum H_2 loading rate obtained in the present study was 10.8 L L_{Rv}^{-1} d^{-1}, which is higher than in many others (7.2–9.9 L_{CH4} L_{Rv}^{-1} d^{-1}); (Porté et al. 2019, Dahl Jønson et al. 2020, Ashraf et al. 2021). Sieborg et al. (2020) found a higher H_2 loading rate of 11.9 L L_{Rv}^{-1} d^{-1} in a thermophilic TBR study, though the CH_4 productivity (2.08 L_{CH4} L_{Rv}^{-1} d^{-1}) and CH_4 content (67 %) were lower than in the present study (2.6 L_{CH4} L_{Rv}^{-1} d^{-1} and 75–86 %). It is noteworthy, however, that to compare reactor BHM performances in different studies, several factors such as the TBR design, operation parameters, inoculum origin and trickling liquid source must be considered.

In practice, the current results show that, for example, in a biogas plant with an anaerobic digestor size of 3000 m^3, biogas productivity of 500 m^3 h^{-1} and approximately 200 m^3 h^{-1} CO_2 (considering 40 % CO_2 in the biogas), a TBR of 8000 m^3 and a GRT of 8 h is required for the BHM process. In contrast, a GRT of

Table 4
TBR performance in thermophilic BHM studies utilizing digestate as inoculum and/or digestate or reject water as trickling liquid.

Inoculum	Trickling liquid	Reactor size (L)	H_2 loading rate (L_{H2} L_{Rv}^{-1} d^{-1})	CH_4 content (%)	CH_4 production rate (L_{CH4} L_{Rv}^{-1} d^{-1})	Reference
Digestate after sieving	Digestate reject water after sieving	8.3	10.8	75–86	2.6	This study
Digestate	Mineral medium	58.1	62.1	98.5	15.4	Strübing et al. (2017)
Digestate, degassed for 4 days	Filtered and pasteurized cattle manure	0.291	11	98	2.53	Dahl Jønson et al. (2020)
Enrichment culture from lab-scale reactor	Pasteurized cattle manure	0.291	11.9	67	2.08	Sieborg et al. (2020)
Enrichment culture from lab-scale reactor	>3 months pre-incubated digestate	1	7.2	95	1.7	Porté et al. (2019)

2 h decreases the reactor size to 2000 m^3, assuming a H_2:CO_2 feeding ratio of 4:1, and requires 800 m^3 h^{-1} of H_2. This results in an additional CH_4 production rate of about 210 m^3 h^{-1}, assuming a H_2 conversion efficiency of 99 %, for an overall CH_4 productivity of 510 m^3 h^{-1} in the combined AD and *ex-situ* BHM. The BHM reaction also produces water of approximately 350 L h^{-1}, or about 1.6 L water per m^3 CH_4 produced (Choi et al. 2019), which could be treated together with other water streams. Adding trace elements during reject water usage in this study helped stabilize the process performance at higher H_2 loading rates. Trace elements are considered essential for enzyme complexes, with their depletion or limitation shown to have a negative impact on process performance (Wintsche et al. 2016). Other BHM studies have also emphasized the importance of trace element addition in *ex-situ* BHM (Strübing et al. 2017, Thapa et al. 2022). Therefore, in planning full-scale processes with other reject water sources, the need for additional nutrients and trace elements must be further investigated.

During the Experimental phase, the total VFA concentrations were 0.9–3.7 g-COD L^{-1}, showing fluctuations. Based on the microbial community analysis results (**see section 3.2**), some of the VFAs could have been converted to CH_4 indirectly. The SAOBs, such as MBA03 and DTU014, oxidized VFAs to H_2/CO_2 and H_2/CO_2 were converted to CH_4 through hydrogenotrophic methanogens. SAOBs are commonly detected in the thermophilic anaerobic digestion of biowaste (Dyksma et al. 2020). This is in line with other studies that have detected VFAs, particularly acetate, during H_2/CO_2 consumption and simultaneous acetate conversion into H_2/CO_2 and methane, indicating syntrophic acetate oxidation followed by methanogenesis (Bassani et al. 2017, Kougias et al. 2017, Porté et al. 2019). In this study, acetate production and consumption were faster during the Experimental phase when compared to the Start-up and Adaptation phases, which could indicate a dynamic, well-enriched microbial community. Alternatively, the anaerobic degradation of residual organic matter in the reject water could have converted to VFAs and biogas, thus reducing the final CH_4 content due to CO_2 production. In this study, H_2:CO_2 was supplied in a theoretical stoichiometric ratio of 4:1, with a H_2 conversion efficiency of close to 100 % and up to 1.8 h in GRT. However, CO_2 conversion efficiency remained at 90–93 %, which could indicate CO_2 production from organic matter in the reject water and lead to a lower average CH_4 content of 80.6 %, still in the threshold requirement of some national gas grids (Muñoz et al. 2015). To increase CH_4 content further and to remove the residual CO_2 originating from the degradation of organic matter in the reject water, H_2 flow rates can be increased to convert the produced CO_2 into CH_4. In a recent study using digestate as a trickling liquid in mesophilic BHM the surplus CO_2 was converted to CH_4 with the H_2:CO_2 stoichiometric ratio of 6:1 (Thapa et al. 2022). Hence, when using digestates or reject water as a nutrient source in BHM, the H_2:CO_2 ratio can be increased above theoretical stoichiometric ratios based on feedstock gases.

While reject water as a trickling liquid in *ex-situ* BHM has the advantage of providing nutrients and, thus, reducing operational costs (compared to a mineral medium), the need for trace element supplementation should be considered and further investigated. While reject waters may lack crucial trace elements, they are diluted during the TBR run, as 1.6 L of water is generated per m^3 CH_4 (Choi et al. 2019). Despite using mineral media as a trickling liquid, Strübing et al. (2017) reported the low levels of sulphide and Fe, Zn, Ni, Na and Co as critical elements in TBRs performing BHM inoculated with digestate. Furthermore, Fe and ammonium were found critical for stable thermophilic *ex-situ* BHM when using pasteurized cow manure as a trickling liquid and nutrient source (Ashraf et al. 2021). Trace elements are essential for enzyme complexes (Wintsche et al. 2016) and play a key role in, for instance, hydrogenotrophic methanogenesis pathways that catalyse redox reactions (Ashraf et al. 2021). As such, their depletion negatively affects process performance. Methanogens are also dependent on Na^+ ions for growth and methane formation mainly by coenzyme M methyltransferase which is involved in CO_2 reduction into methane and acetate (Perski et al. 1982). The concentration of Na^+ has been closely monitored in the current study and no limitations were detected (Fig. 3 **d**). Despite the high ammonium content (2.5 ± 0.15 g L^{-1}) in this study's reject water, the ammonium concentration in the trickling liquid remained at 1.0–1.5 g L^{-1} (Fig. 3**c and d**) during the Experimental phase, and it was determined to have no inhibitory impact. It is noteworthy that reject water characteristics are very much case dependent, and while in this study the addition of trace elements was necessary to facilitate stable process performance at higher H_2 loading rates, other reject water screening studies are needed to fully assess their suitability as a nutrient source in BHM processes.

4.3. Microbial community dynamics

This study's results show that increasing H_2 loading rate successfully increases the relative abundance of hydrogenotrophic methanogens in *ex-situ* TBRs, while the switch from a mineral medium to reject water had a smaller effect. The relative abundance of archaea in the TBRs (up to 67 %) was much higher than in a previous study with a maximum 30 % relative abundance in thermophilic BHM using digestate as a trickling liquid (Dupnock et al. 2017, Porté et al. 2019). Even though the archaeal communities were evolving during the Start-up and Adaptation phases, the conditions of the Experimental phase were more selective for the enrichment of methanogenic archaea. The shift in alpha diversity also indicated selectivity: significantly decreased evenness in both biofilm and planktonic communities and significantly decreased richness in the biofilm community in the Experimental phase occurred compared to the Start-up and Adaptation phases. The selective conditions, such as increased H_2 loading rates, also showed selective pressure towards the enrichment of hydrogenotrophic methanogens in both the biofilm and trickling liquid. This agrees with previous studies which observed that under thermophilic conditions using digestate or cow manure as a trickling liquid, TBRs select hydrogenotrophic methanogens, mainly from the *Methanothermobacter* genus (Bassani et al. 2017, Porté et al. 2019, Dahl Jønson et al. 2020). However, in this study the relative abundance of hydrogenotrophic methanogen (up to 67 % in the biofilm samples) was much higher than in extant studies. This could be due to selective conditions created from increasing H_2 loading rates and the crucial macronutrients provided by the reject water and added trace elements.

The most abundant bacterial genus in this study was *Defluviitoga*, which has been widely reported in thermophilic AD plants and is attributed to converting sugars into H_2/CO_2 (Ao et al. 2019, Li et al. 2022). This genus also has a role in the hydrolysis of complex materials, such as cellulose, xylan and chitin (Maus et al. 2016). The increased abundance of this genus in the current study can be attributed to the presence of hardly any biodegradable material in the biowaste digestate and reject water used as the inoculum and nutrient source, respectively. MBA03 is a SAOB and has been reported in thermophilic *in-situ* BHM processes (Zhu et al. 2019, Xie et al. 2021), as well as in AD processes using food and silage waste and cattle manure (Braga Nan et al. 2020). The relatively high abundance of MBA03 in the planktonic samples during the acetate degradation periods of the Adaptation (16 ± 6 %) and Experimental phases (14 ± 3 %) might indicate its role in acetate oxidation to H_2/CO_2. Kougias et al. (2017) and Porté et al. (2019) reported the enrichment of *Bacillus* species in biofilm and planktonic samples in BHM processes, and hypothesized them to

perform interspecies extracellular electron transfers with archaea to balance redox reactions at exergonic levels in thermophilic biogas upgrading systems. The *Acetomicrobium* genus is widely reported in biogas production reactors, and their role could be attributed to the digestion of fats and proteins (Litti et al. 2021), as well as glucose fermentation to acetate, CO_2 and H_2 (Hania et al. 2016). During periods of acetate accumulation in this study's TBRs, simultaneous increases in the relative abundance of this species was evident (Fig. 3**b and 5**). The syntrophic association of hydrogenotrophic methanogens (particularly *Methanobacterium*) with acidogenic bacteria such as *Defluviitoga* and *Acetomicrobium*, as well as with fermentative and acetate oxidizing bacteria such as MBA03, *Gleria* and DTU014, as evidenced in this study, has been previously reported in anaerobic thermophilic methanation processes (Zhu et al. 2019, Li et al. 2022). Accordingly, acetate produced from the residual organic matter in the reject water by hydrolytic and fermentative bacteria may have been oxidized by SAOBs to H_2 and CO_2 (Fig. 3**b**), then further converted to CH_4 by hydrogenotrophic methanogens. These dynamics may explain the higher CH_4 yield compared to H_2 and CO_2 conversion efficiencies (Table 3).

5. Conclusions

Thermophilic *ex-situ* BHM appears feasible for integration into biogas plants by utilizing reject water as a trickling liquid, while the use of digestate as an inoculum requires further study to enable shorter start-up periods. A H_2 conversion of more than 95 % was achieved at a H_2 loading rate of 10.8 $L_{H2}\ L_{Rv}^{-1}\ d^{-1}$, resulting in the CH_4 production rate of 2.6 $L\ L_{Rv}^{-1}\ d^{-1}$. Switching from a mineral medium to reject water with high VFAs and ammonium concentration of 2.2 $g\ L^{-1}$ was not inhibitory to the methanogenic community. The addition of trace elements to reject water at higher GLRs was crucial to maintain high H_2 conversion efficiency and methane yield. Use of reject water and increasing H_2 loading rate appeared effective in enriching hydrogenotrophic methanogens attaining relative abundance of up to 67 %.

Author contributions.

DK, MK, JK, AM and MS conceptualized the study and planned the experiments. DK and MK designed the BHM process and bioreactors. DK performed the bioreactor cultivations, analytics, and data analysis, as well as the visualization, and wrote the first draft of the manuscript. JRK performed the bioinformatics data analysis. HAL supported the elemental analysis measurements and data analysis. JK and MK performed the project administration and supervised the study. AM and MS provided the study's funding and resources. DK, JK, MK and JRK reviewed and edited the manuscript. All authors read and approved the final manuscript.

Availability of data and materials

The data sets supporting the conclusions of this article are included in the main article as well as the supplementary data. The raw data are to remain confidential and will not be shared.

Data availability

Data will be made available on request.

Declaration of Competing Interest

The authors declare that they have no known competing financial interests or personal relationships that could have appeared to influence the work reported in this paper.

Acknowledgments

The financial support of Doranova Ltd. is gratefully acknowledged. Antti Nuottajärvi and Mika Karttunen are also acknowledged for their support in the laboratory.

Appendix A. Supplementary data

Supplementary data to this article can be found online at https://doi.org/10.1016/j.ces.2023.118498.

References

Alitalo, A., Niskanen, M., Aura, E., 2015. Biocatalytic methanation of hydrogen and carbon dioxide in a fixed bed bioreactor. Bioresour. Technol. 196, 600–605.
Ao, T., Li, R., Chen, Y., Li, C., Li, Z., Liu, X., Ran, Y., Li, D., 2019. Anaerobic thermophilic digestion of maotai-flavored distiller's grains: process performance and microbial community dynamics. Energy Fuels 33 (9), 8804–8811.
APHA (2018). 5220 CHEMICAL OXYGEN DEMAND (COD). Standard Methods For the Examination of Water and Wastewater, American Public Health Association.
APHA (2018). 2540 SOLIDS. Standard Methods For the Examination of Water and Wastewater. B. T. Lipps WC, Braun-Howland E, editors.
Ashraf, M.T., Yde, L., Triolo, J.M., Wenzel, H., 2021. Optimizing the dosing and trickling of nutrient media for thermophilic biomethanation in a biotrickling filter. Biochem. Eng. J. 176, 108220.
Baleeiro, F.C.F., Kleinsteuber, S., Sträuber, H., 2021. Hydrogen as a Co-electron Donor for Chain Elongation With Complex Communities. Front. Bioeng, BioSci, p. 9.
Bassani, I., Kougias, P.G., Treu, L., Porté, H., Campanaro, S., Angelidaki, I., 2017. Optimization of hydrogen dispersion in thermophilic up-flow reactors for ex situ biogas upgrading. Bioresour. Technol. 234, 310–319.
Bolyen, E., Rideout, J.R., Dillon, M.R., Bokulich, N.A., Abnet, C.C., Al-Ghalith, G.A., Alexander, H., Alm, E.J., Arumugam, M., Asnicar, F., 2019. Reproducible, interactive, scalable and extensible microbiome data science using QIIME 2. Nat. Biotechnol. 37 (8), 852–857.
Braga Nan, L., Trably, E., Santa-Catalina, G., Bernet, N., Delgenès, J.-P., Escudié, R., 2020. Biomethanation processes: new insights on the effect of a high H2 partial pressure on microbial communities. Biotechnol. Biofuel. 13 (1), 141.
Burkhardt, M., Jordan, I., Heinrich, S., Behrens, J., Ziesche, A., Busch, G., 2019. Long term and demand-oriented biocatalytic synthesis of highly concentrated methane in a trickle bed reactor. App. Energy 240, 818–826.
Choi, O., Kim, M., Go, Y., Hong, M.-G., Kim, B., Shin, Y., Lee, S., Kim, Y.G., Joo, J.S., Jeon, B.S., Sang, B.-I., 2019. Selective Removal of Water Generated during Hydrogenotrophic Methanation from Culture Medium Using Membrane Distillation. Energies 12 (21), 4130.
Dahl Jønson, B., Ujarak Sieborg, M., Tahir Ashraf, M., Yde, L., Shin, J., Shin, S.G., Mi Triolo, J., 2020. Direct inoculation of a biotrickling filter for hydrogenotrophic methanogenesis. Bioresour. Technol. 318, 124098.
Dupnock, T.L., Deshusses, M.A., 2017. High-Performance Biogas Upgrading Using a Biotrickling Filter and Hydrogenotrophic Methanogens. Appl. Biochem. Biotechnol. 183 (2), 488–502.
Dyksma, S., Jansen, L., Gallert, C., 2020. Syntrophic acetate oxidation replaces acetoclastic methanogenesis during thermophilic digestion of biowaste. Microbiome 8 (1), 105.
Gavala, H.N., Grimalt-Alemany, A., Asimakopoulos, K., Skiadas, I.V., 2021. Gas Biological Conversions: The Potential of Syngas and Carbon Dioxide as Production Platforms. Waste Biomass Valori. 12 (10), 5303–5328.
Hania, W.B., Bouanane-Darenfed, A., Cayol, J.-L., Ollivier, B., Fardeau, M.-L., 2016. Reclassification of Anaerobaculum mobile, Anaerobaculum thermoterrenum, Anaerobaculum hydrogeniformans as Acetomicrobium mobile comb. nov., Acetomicrobium thermoterrenum comb. nov. and Acetomicrobium hydrogeniformans comb. nov., respectively, and emendation of the genus Acetomicrobium. Int. J. Syst. Evol. Microbiol. 66 (3), 1506–1509.
Jensen, M.B., Strübing, D., de Jonge, N., Nielsen, J.L., Ottosen, L.D.M., Koch, K., Kofoed, M.V.W., 2019. Stick or leave–Pushing methanogens to biofilm formation for ex situ biomethanation. Bioresour. Technol. 291, 121784.
Jønson, B.D., Tsapekos, P., Tahir Ashraf, M., Jeppesen, M., Ejbye Schmidt, J., Bastidas-Oyanedel, J.-R., 2022. Pilot-scale study of biomethanation in biological trickle bed reactors converting impure CO2 from a Full-scale biogas plant. Bioresour. Technol. 365, 128160.
Kokko, M., Koskue, V., Rintala, J., 2018. Anaerobic digestion of 30–100-year-old boreal lake sedimented fibre from the pulp industry: Extrapolating methane production potential to a practical scale. Water Res. 133, 218–226.
Kougias, P.G., Treu, L., Benavente, D.P., Boe, K., Campanaro, S., Angelidaki, I., 2017. Ex-situ biogas upgrading and enhancement in different reactor systems. Bioresour. Technol. 225, 429–437.
Li, C., He, P., Hao, L., Lü, F., Shao, L., Zhang, H., 2022. Diverse acetate-oxidizing syntrophs contributing to biogas production from food waste in full-scale anaerobic digesters in China. Renew. Energy 193, 240–250.
Litti, Y.V., Kovalev, D., Kovalev, A., Merkel, A.Y., Vishnyakova, A., Russkova, Y.I., Nozhevnikova, A., 2021. Auto-selection of microorganisms of sewage sludge

used as an inoculum for fermentative hydrogen production from different substrates. Int. J. Hydrogen Energy 46 (58), 29834–29845.
Luo, G., Angelidaki, I., 2012. Integrated biogas upgrading and hydrogen utilization in an anaerobic reactor containing enriched hydrogenotrophic methanogenic culture. Biotechnol. Bioeng. 109 (11), 2729–2736.
Maegaard, K., Garcia-Robledo, E., Kofoed, M.V., Agneessens, L.M., de Jonge, N., Nielsen, J.L., Ottosen, L.D., Nielsen, L.P., Revsbech, N.P., 2019. Biogas upgrading with hydrogenotrophic methanogenic biofilms. Bioresour. Technol. 287, 121422.
Maus, I., Cibis, K.G., Bremges, A., Stolze, Y., Wibberg, D., Tomazetto, G., Blom, J., Sczyrba, A., König, H., Pühler, A., 2016. Genomic characterization of Defluviitoga tunisiensis L3, a key hydrolytic bacterium in a thermophilic biogas plant and its abundance as determined by metagenome fragment recruitment. J. Biotechnol. 232, 50–60.
Muñoz, R., Meier, L., Diaz, I., Jeison, D., 2015. A review on the state-of-the-art of physical/chemical and biological technologies for biogas upgrading. Rev. Environ. Sci. Biotechnol. 14 (4), 727–759.
Owen, W., Stuckey, D., Healy Jr, J., Young, L., McCarty, P., 1979. Bioassay for monitoring biochemical methane potential and anaerobic toxicity. Water Res. 13 (6), 485–492.
Ozturk, M., Dincer, I., 2021. A comprehensive review on power-to-gas with hydrogen options for cleaner applications. Int. J. Hydrogen Energy 46 (62), 31511–31522.
Perski, H.J., Schönheit, P., Thauer, R.K., 1982. Sodium dependence of methane formation in methanogenic bacteria. FEBS Lett. 143 (2), 323–326.
Porté, H., Kougias, P.G., Alfaro, N., Treu, L., Campanaro, S., Angelidaki, I., 2019. Process performance and microbial community structure in thermophilic trickling biofilter reactors for biogas upgrading. Sci. Total Environ. 655, 529–538.
Rachbauer, L., Voitl, G., Bochmann, G., Fuchs, W., 2016. Biological biogas upgrading capacity of a hydrogenotrophic community in a trickle-bed reactor. App. Energy 180, 483–490.
Rafrafi, Y., Laguillaumie, L., Dumas, C., 2021. Biological Methanation of H2 and CO2 with Mixed Cultures: Current Advances, Hurdles and Challenges. Waste Biomass Valori. 12 (10), 5259–5282.
Rittmann, S., Seifert, A., Herwig, C., 2015. Essential prerequisites for successful bioprocess development of biological CH4 production from CO2 and H2. Crit. Rev. Biotechnol. 35 (2), 141–151.
Rusmanis, D., O'Shea, R., Wall, D.M., Murphy, J.D., 2019. Biological hydrogen methanation systems–an overview of design and efficiency. Bioengineered 10 (1), 604–634.
Sieborg, M.U., Jønson, B.D., Ashraf, M.T., Yde, L., Triolo, J.M., 2020. Biomethanation in a thermophilic biotrickling filter using cattle manure as nutrient media. Bioresource Technol. Report. 9, 100391.
Sposob, M., Wahid, R., Fischer, K., 2021. Ex-situ biological CO2 methanation using trickle bed reactor: review and recent advances. Rev. Environ. Sci. Biotechnol. 20 (4), 1087–1102.
Strübing, D., Huber, B., Lebuhn, M., Drewes, J.E., Koch, K., 2017. High performance biological methanation in a thermophilic anaerobic trickle bed reactor. Bioresour. Technol. 245, 1176–1183.
Strübing, D., Moeller, A.B., Mößnang, B., Lebuhn, M., Drewes, J.E., Koch, K., 2018. Anaerobic thermophilic trickle bed reactor as a promising technology for flexible and demand-oriented H2/CO2 biomethanation. App. Energy 232, 543–554.
Strübing, D., Moeller, A.B., Mößnang, B., Lebuhn, M., Drewes, J.E., Koch, K., 2019. Load change capability of an anaerobic thermophilic trickle bed reactor for dynamic H2/CO2 biomethanation. Bioresour. Technol. 289, 121735.
Tampio, E., Ervasti, S., Paavola, T., Heaven, S., Banks, C., Rintala, J., 2014. Anaerobic digestion of autoclaved and untreated food waste. Waste Management 34 (2), 370–377.
Thapa, A., Park, J.-G., Jun, H.-B., 2022. Enhanced ex-situ biomethanation of hydrogen and carbon dioxide in a trickling filter bed reactor. Biochem. Eng. J. 179, 108311.
Wintsche, B., Glaser, K., Sträuber, H., Centler, F., Liebetrau, J., Harms, H., Kleinsteuber, S., 2016. Trace elements induce predominance among methanogenic activity in anaerobic digestion. Front. Microbiol. 7, 2034.
Xie, Z., Meng, X., Ding, H., Cao, Q., Chen, Y., Liu, X., Li, D., 2021. The synergistic effect of rumen cellulolytic bacteria and activated carbon on thermophilic digestion of cornstalk. Bioresour. Technol. 338, 125566.
Zhu, X., Chen, L., Chen, Y., Cao, Q., Liu, X., Li, D., 2019. Differences of methanogenesis between mesophilic and thermophilic in situ biogas-upgrading systems by hydrogen addition. J. Industrial Microb. and Biotechnol. 46 (11), 1569–1581.